

Electronic Supplementary Information

Distinctive Optical Transitions of Tunable Multicolor Carbon Dots

Hyeong Seop Shim, Jun Myung Kim, Seonghyun Jeong, Youngwon Ju, Sung Jae Won,
Jeongyun Choi, Sangwon Nam, Aniruddha Molla, Joocheon Kim,* and Jae Kyu Song*

Department of Chemistry, Kyung Hee University, Seoul 02447, Republic of Korea

*Corresponding authors. E-mail addresses: jkim94@khu.ac.kr, jaeksong@khu.ac.kr

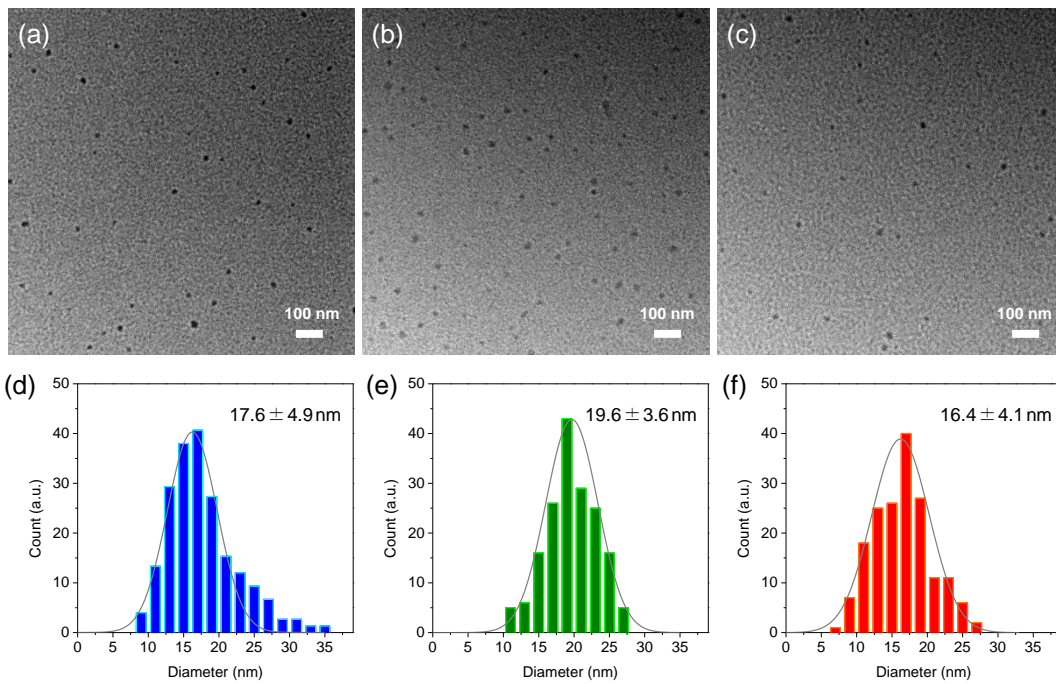


Figure S1. TEM images of (a) MCD, (b) OCD, and (c) PCD. The size distributions of (d) MCD, (e) OCD, and (f) PCD measured by TEM.

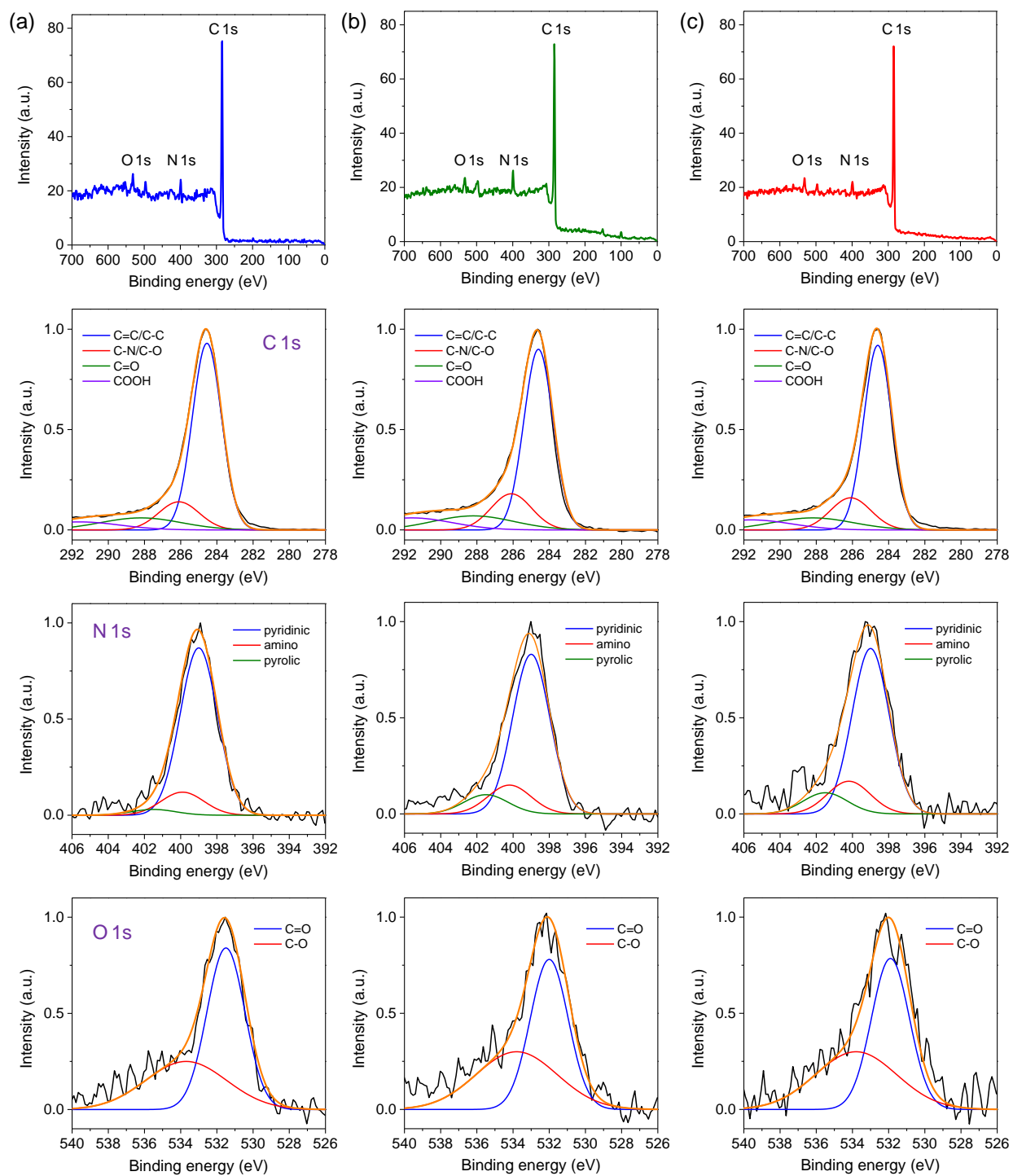


Figure S2. XPS spectra of (a) MCD, (b) OCD, and (c) PCD.

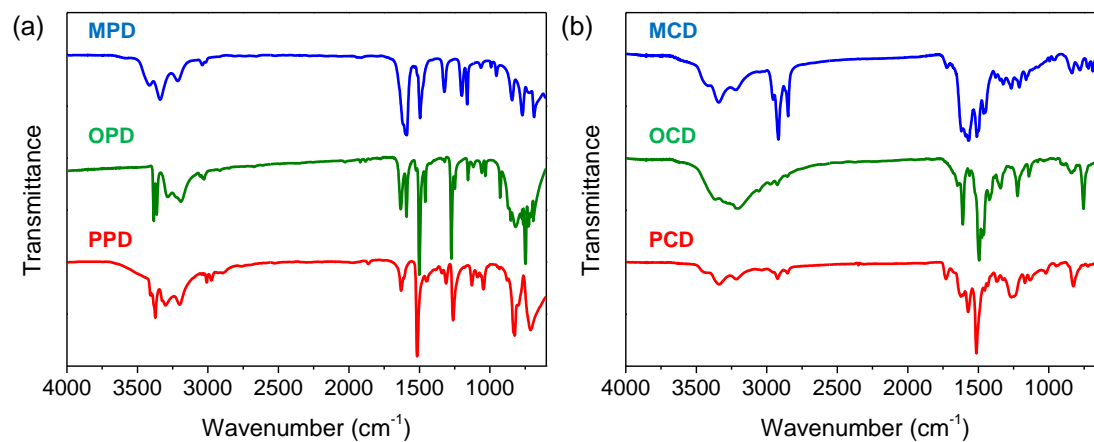


Figure S3. FTIR spectra of (a) PDs and (b) CDs.

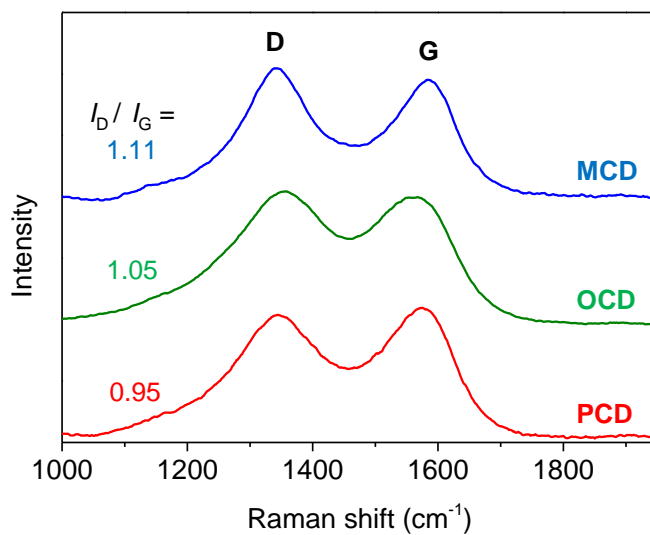


Figure S4. Raman spectra of CDs show the D-band at 1350 cm^{-1} and G-band at 1580 cm^{-1} . The intensity ratio of two bands (I_D/I_G) is in the range of 0.95–1.11.

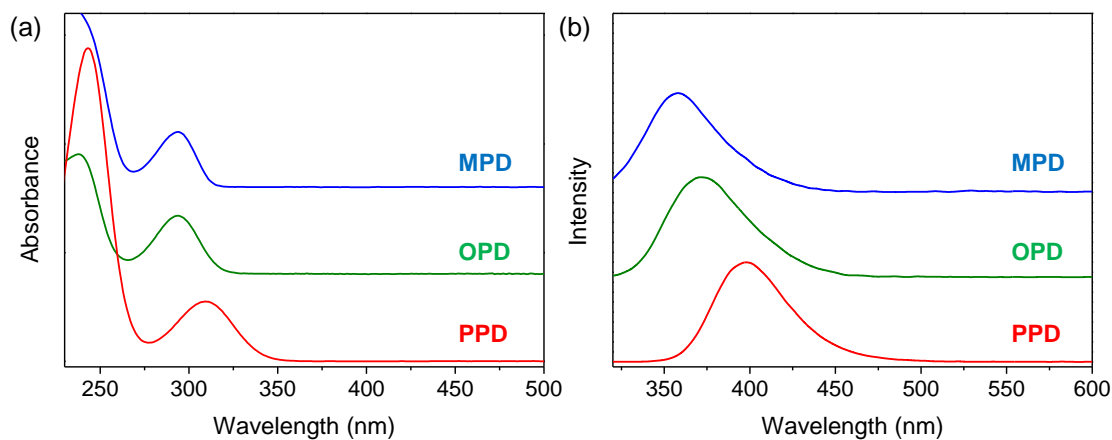


Figure S5. (a) Absorption and (b) PL spectra of PDs.

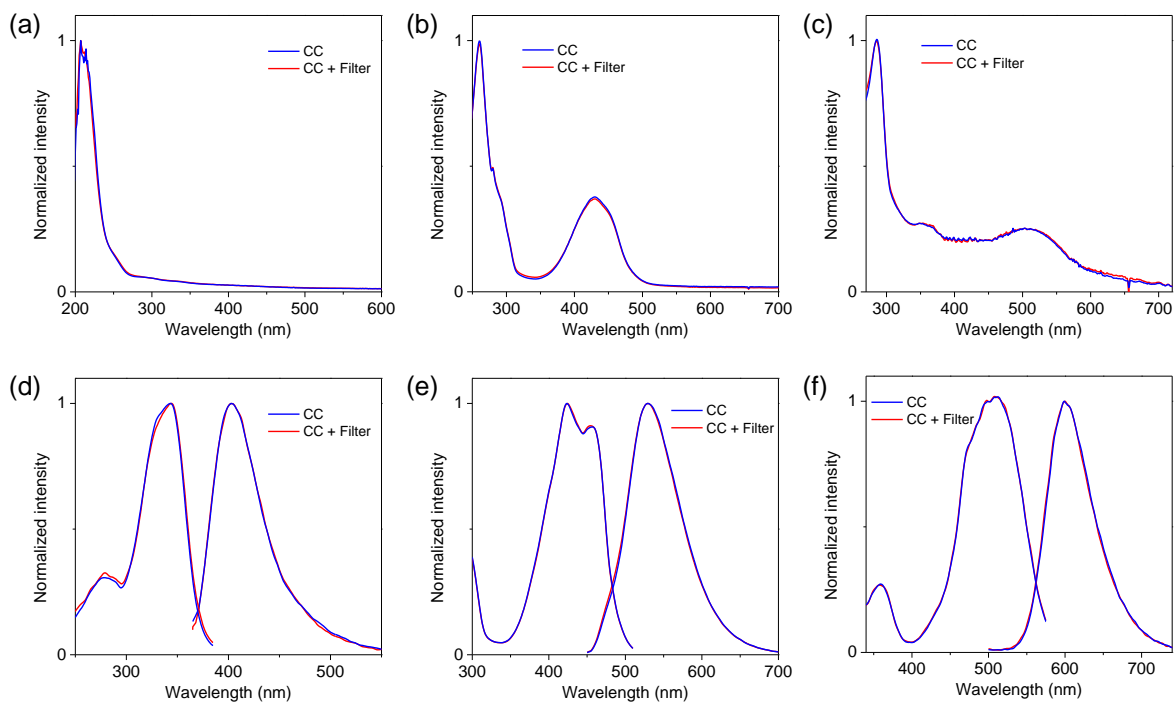


Figure S6. Absorption spectra of (a) BCD, (b) GCD, and (c) RCD purified by both silica gel column chromatography and ultrafiltration (CC + Filter) are compared to those by the silica gel column chromatography (CC). Photoluminescence excitation and photoluminescence spectra of (d) BCD, (e) GCD, and (f) RCD purified by both silica gel column chromatography and ultrafiltration (CC + Filter) are compared to those by the silica gel column chromatography (CC).

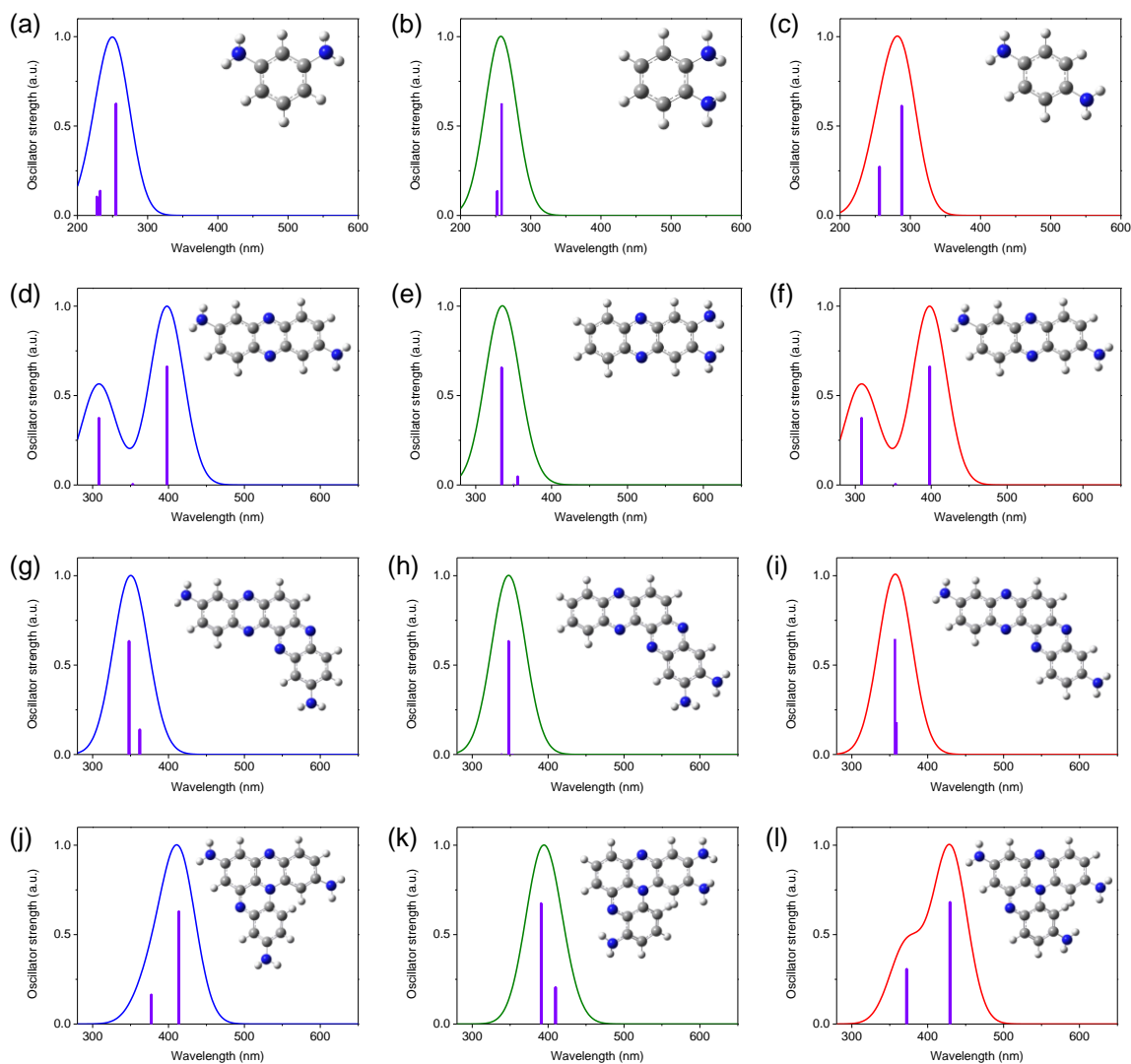


Figure S7. The calculated absorption spectra of monomeric forms of (a) MPD, (b) OPD, and (c) PPD. Carbon, nitrogen, and hydrogen atoms are denoted as gray, blue, and light gray colors, respectively. The calculated spectra of dimeric forms of (d) MPD, (e) OPD, and (f) PPD. The calculated spectra of bent trimeric forms of (g) MPD, (h) OPD, and (i) PPD. The calculated spectra of planar trimeric forms of (j) MPD, (k) OPD, and (l) PPD. Insets show the stable geometries.

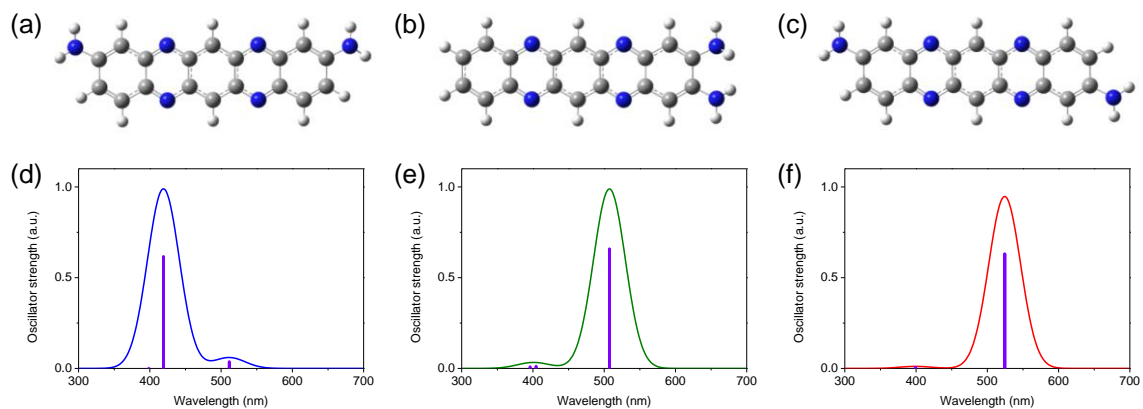


Figure S8. The calculated stable geometries of trimeric forms of (a) MPD, (b) OPD, and (c) PPD. Carbon, nitrogen, and hydrogen atoms are denoted as gray, blue, and light gray colors, respectively. The corresponding calculated absorption spectra of trimeric forms of (d) MPD, (e) OPD, and (f) PPD.

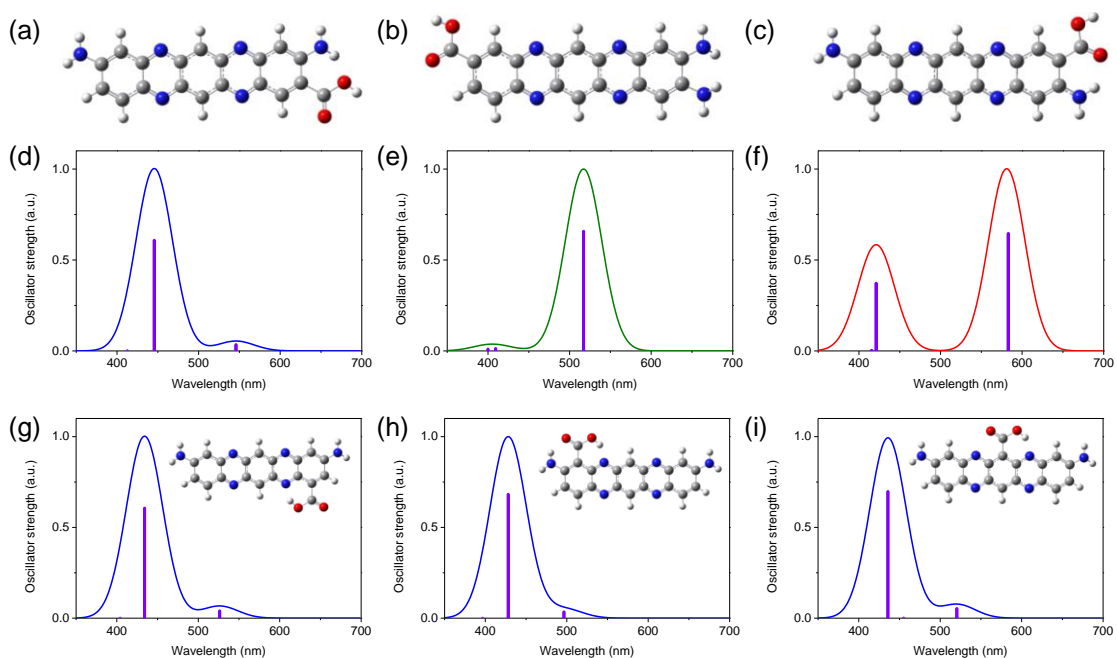


Figure S9. The calculated stable geometries of trimeric forms of (a) MPD, (b) OPD, and (c) PPD with a carboxyl group. Carbon, nitrogen, hydrogen, and oxygen atoms are denoted as gray, blue, light gray, and red colors, respectively. The corresponding calculated absorption spectra of (d) MPD, (e) OPD, and (f) PPD. (g)-(i) The calculated absorption spectra of trimeric forms of MPD with different positions of a carboxyl group. Insets show the stable geometries.

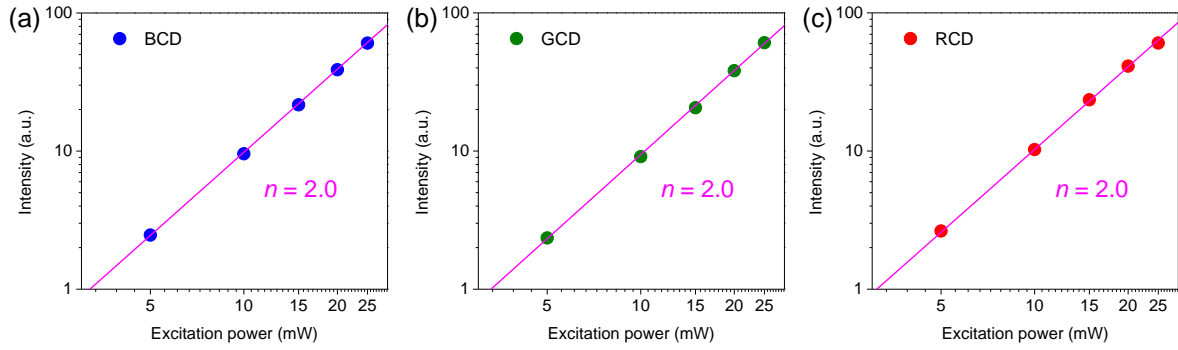


Figure S10. Integrated emission intensities of TPL in (a) BCD, (b) GCD, and (c) RCD show the quadratic dependence on excitation intensities. The lines of $n = 2$ in the relation of $I_{\text{PL}} = a I_{\text{ex}}^n$ are plotted for comparison.

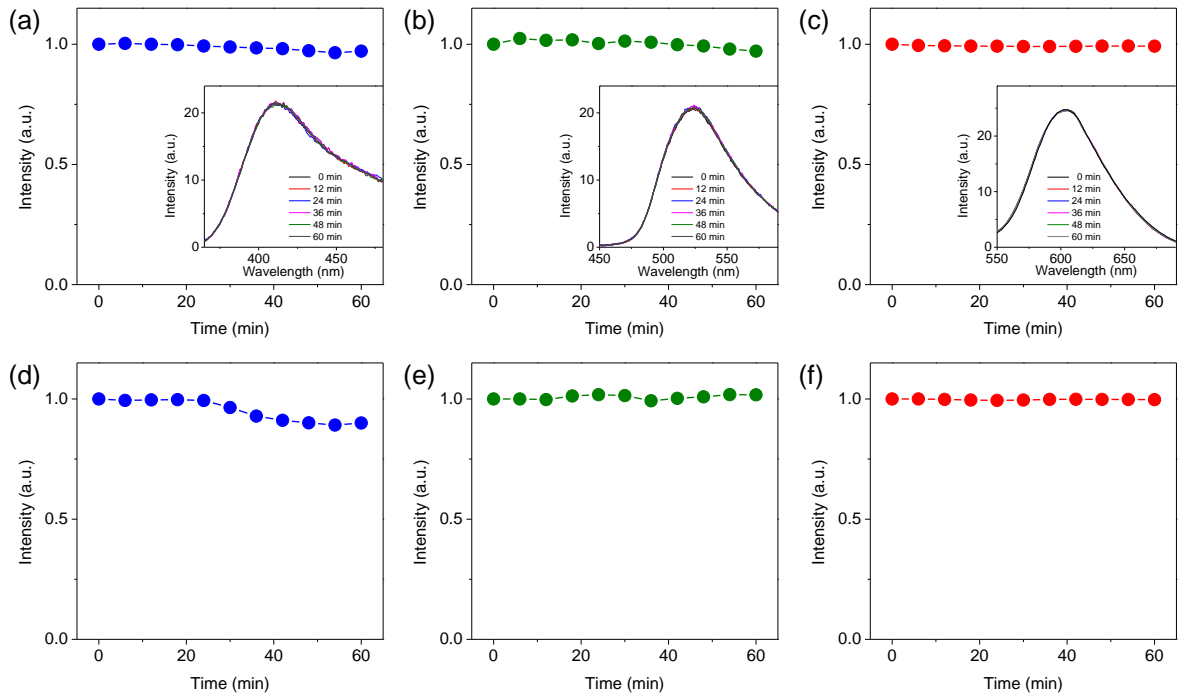


Figure S11. Integrated emission intensities of TPL in (a) BCD, (b) GCD, and (c) RCD, while being exposed to pulsed excitation of near-IR (710 nm) at a high repetition rate (1.0×10^6 Hz) and a high excitation intensity ($50 \mu\text{J}/\text{cm}^2\cdot\text{pulse}$) under ambient conditions. Insets show TPL spectra with increasing exposure time. Integrated emission intensities of the typical PL in (d) BCD, (e) GCD, and (f) RCD, while being exposed to UV (355 nm) at the excitation power of $1.0 \text{ W}/\text{cm}^2$.

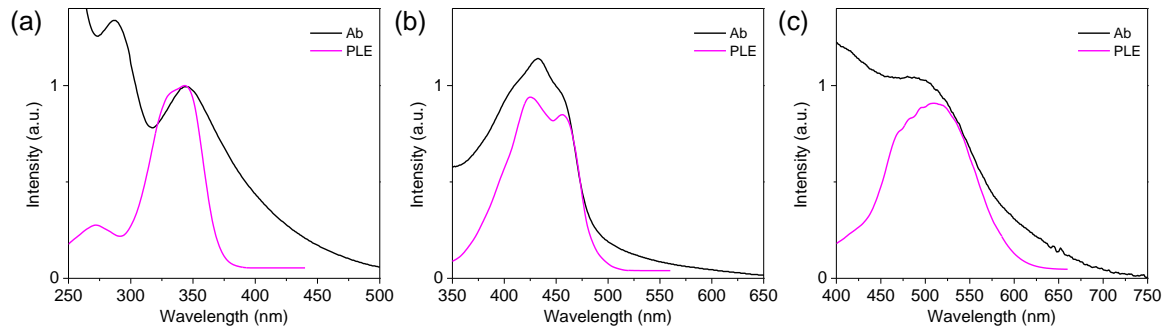


Figure S12. Absorption (Ab) spectra of (a) BCD, (b) GCD, and (c) RCD are compared to photoluminescence excitation (PLE) spectra. The intensities are adjusted for better comparison.

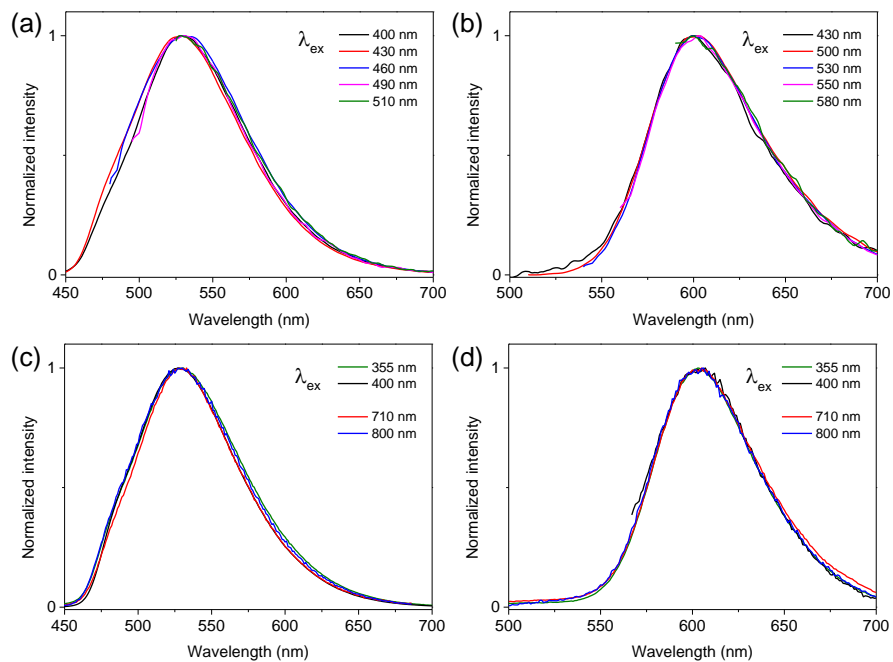


Figure S13. PL spectra of (a) GCD and (b) RCD with increasing excitation wavelength to the tail region of absorption. Emission spectra of (c) GCD and (d) RCD at various excitation wavelengths.